Dielectric Relaxation in Disordered Poly(isoprene–styrene) Diblock Copolymers near the Microphase-Separation Transition

I. Alig,[†,‡] F. Kremer,*[,‡] G. Fytas,[§] and J. Roovers[∥]

Max-Planck-Institut für Polymerforschung, P.O. Box 3148, W-6500 Mainz, Germany, Research Center of Crete, P.O. Box 1527, 71110 Heraklion, Crete, Greece, and Institute of Environmental Chemistry, National Research Council of Canada, Ottawa, K1A 0R6 Canada

Received March 5, 1992; Revised Manuscript Received May 22, 1992

ABSTRACT: Broad-band dielectric spectroscopy (10^{-2}–10^{6} Hz) was employed to investigate molecular dynamics in polyisoprene–polystyrene (PI-*b*-PS) diblock copolymers with different contents of PI varying from 27.9 to 50.4 wt % and having an identical molecular weight of the PS blocks (2830). The diblock copolymers studied were considered to be thermodynamically homogeneous concerning DSC measurements and having a value of χN from 5.5 to 8.9 at 25 °C, where χ is the segment–segment interaction parameter and N the number of statistical segments per chain. Two relaxation processes are observed which sense the molecular dynamics of the PI chain in the diblock copolymer on two different length and time scales: The segmental relaxation is a local process corresponding to the primary relaxation of the PI chain in the PI-rich regions of the thermodynamically homogeneous phase. In contrast, the normal-mode relaxation is assumed to be mainly controlled by an effective friction coefficient reflecting the properties of both block components. The normal-model relaxation in its temperature dependence and in its distribution of relaxation times provides evidence for the coupling to composition fluctuations. Furthermore, there is a hint that the freezing-in of PS segmental fluctuations affects the normal-mode dynamics of the PI blocks. Our results are compared to similar investigations by Yao et al.[13] on PI-*b*-PS under conditions of microphase separation. The findings are consistent with the fluctuation picture recently developed by Fredrickson et al. for diblock copolymers near the microphase-separation transition.

I. Introduction

In the last decade, there has been an increasing interest in block copolymers.[1] Most of the published work deals with static properties in the ordered and disordered phase near the microphase-separation transition (MST) of diblock copolymer melts. The order-to-disorder transition in these systems is a result of a delicate balance between contradicting thermodynamic forces expressed in the reduced quantity χN, where χ is the Flory parameter describing the enthalpic interactions between statistical segments of types A and B. N is the total number of statistical segments per molecule. The equilibrium thermodynamic state of an A–B diblock copolymer melt is then determined by χN and the composition $f = N_A/N$, where N_A is the number of segments of type A in the chain. For values of χN greater than $(\chi N)_t$, for which the MST occurs, the diblock copolymers (A–B) form different microdomain structures depending on f, whereas for $\chi N < (\chi N)_t$, entropic effects dominate and hence A–B is considered to form a homogeneous phase.

For symmetric diblock copolymers ($f = 0.5$), the mean-field theory[2] predicts a critical value $(\chi N)_s = 10.495$ for the spinodal point. In a more recent correction, Fredrickson and Helfand[3] implemented the effect of composition fluctuations on the diblock phase diagram. They replaced the mean-field critical point for $f = 0.5$ by $(\chi N)_s = 10.495 + 41.022N^{-1/3}$, which recovers the mean-field result for $N \to \infty$. Block copolymer melts in the disordered phase display a single glass transition when measured by bulk experimental techniques such as differential scanning calorimetry, suggesting spatial homogeneity down to about 100 Å. Compatibility at shorter length scales can be revealed by probing local molecular motions. Segmental dynamics can then be used to sense effects of the composition fluctuations; $\psi(\vec{r}) = \rho_A(\vec{r})/\bar{\rho} - f$ denotes an order parameter where $\rho_A(\vec{r})$ is the number density of segments A at the point $\vec{r}$ and $\bar{\rho}$ the overall (A + B) segment density. In the frame of the mean-field theory[2] $\langle\psi(\vec{r})\rangle$ is assumed to be uniform and to vanish for all points in the ordered phase.

Dielectric spectroscopy[4] on 1,4-polybutadiene/1,2-polybutadiene diblock copolymers provides evidence of local concentration heterogeneities, being large enough to display a primary relaxation for each of the blocks, even for samples that are considered to be homogeneous on the molecular length scale probed by small-angle neutron scattering. Very recent[5,6] depolarized Rayleigh scattering (DRS) and dielectric spectroscopy (DS) studies of the segmental dynamics of athermal ($\chi = 0$) polyisoprene-*b*-poly(1,2-butadiene) (PI–PVE) copolymer near its glass transition T_g and of a polyisoprene-*b*-polystyrene (PI–PS) melt with $f_{PI} = 0.61$ give further support to local inhomogeneities of A and B blocks in the disordered phase.[3,7–9] In the fluctuation picture[3] of block copolymer melts significant amounts of composition fluctuations are possible in the disordered phase. The amplitude of these fluctuations is assumed to increase with increasing χN.

One possible way for probing the length and time scales of these fluctuations is relaxation studies. Dielectric spectroscopy on copolymers containing type A[10–13] polymers, such as poly(*cis*-1,4-isoprene), offers the possibility to investigate both the collective and the local dynamics with the same method. The former is dielectrically observable due to the nonvanishing dipole component parallel to the chain contour (normal mode), while the latter corresponds to fluctuations of the perpendicular component (segmental mode) of the net dipole moment. Retardation and broadening of the dielectric normal modes of PI blocks in microphase-separated PI-*b*-PS with glassy PS blocks ($T < T_g$(PS)) as compared to PI homopolymers were recently reported.[13] These interesting differences were considered to arise from the confinement of the mobile PI blocks in the microdomain region with frozen PS walls.

In this paper we present DS results for both local (segmental) and large-scale (normal) chain motion in three

† Permanent address: Institut für Physikalische Chemie, Universität zu Köln, Luxemburger Strasse 116, W-5000 Köln 41, Germany.
‡ Max-Planck-Institut für Polymerforschung.
§ Research Center of Crete.
∥ National Research Council of Canada.

0024-9297/92/2225-5277$03.00/0

polyisoprene-*b*-polystyrene (PI-*b*-PS) samples in the disordered state; χN at 25 °C varies between 5.5 and 8.9. The samples are thermodynamically homogeneous, having one (broadened) glass transition.

II. Theoretical Background

The complex dielectric permittivity $\epsilon^*(\omega) = \epsilon'(\omega) - i\epsilon''(\omega)$ of a macroscopic system is provided by the one-sided Fourier or pure imaginary Laplace transform of the time derivative of the normalized response function $\Phi(t)$ for the dielectric polarization of the system[14-16]

$$\frac{\epsilon^*(\omega) - \epsilon_\infty}{\epsilon_s - \epsilon_\infty} = \int_0^\infty \exp[-i\omega t]\left[-\frac{d\Phi(t)}{dt}\right] dt \qquad (1)$$

where ϵ_s and ϵ_∞ are the limiting low- and high-frequency permittivities, respectively. The dielectric response of the PI-*b*-PS copolymer mainly originates in the contribution of PI because the dielectric strength of PS is about 2 times smaller than that of PI. For the PI blocks the response function $\Phi(t)$ can be decomposed into contributions of dipole moment components parallel μ'' and perpendicular $\mu^\perp$ to the chain contour.[10-12] When neglecting cross correlations between segments of different chains, the autocorrelation $\Phi(t)$ for the ith chain can be written as

$$\Phi(t) = \frac{\sum_i \sum_l \langle \mu''_{ij}(0)\, \mu''_{il}(t)\rangle + \sum_i \sum_l \langle \mu^\perp_{ij}(0)\, \mu^\perp_{il}(t)\rangle}{\sum_j \sum_l \langle \mu''_{ij}(0)\, \mu''_{il}(0)\rangle + \sum_j \sum_l \langle \mu^\perp_{ij}(0)\, \mu^\perp_{il}(0)\rangle} \qquad (2)$$

where $\langle \mu''_{il}(0)\, \mu''_{il}(t)\rangle$ is the end-to-end or "graft end"-to-end vector autocorrelation function, respectively, for the ith chain at time t. The first term in eq 2 can be rewritten as

$$\sum_j \sum_l \langle \mu''_{ij}(0)\, \mu''_{il}(t)\rangle = \mu^2 \langle \mathbf{r}_i(0)\, \mathbf{r}_i(t)\rangle \qquad (3)$$

where μ is the absolute value of the parallel component of the dipole moment per unit contour length; $\mathbf{r}_i(t)$ is the end-to-end or "graft end"-to-end vector for the ith chain. The second term of eq 2 is simply reduced to the autocorrelation function of the perpendicular dipole moment component representing segmental motions which can sense the local structure of block copolymers.[5,6,13] If the relaxation times for the two components of $\Phi(t)$ are well apart in the time domain, the individual autocorrelation functions can be separated.

For nonentangled linear bulk polymers, $\langle \mathbf{r}_i(0)\, \mathbf{r}_i(t)\rangle$ is expressed by the Rouse free-draining model:[10,17]

$$\langle \mathbf{r}_i(0)\, \mathbf{r}_i(t)\rangle / \langle r^2\rangle = (8/\pi^2) \sum_p (1/p^2) \exp(-t/\tau_p) \qquad (4)$$

$$\tau_p = \frac{\zeta N^2 b^2}{3\pi^2 k T p^2} \qquad p = 1, 3, 5, \ldots \qquad (5)$$

where τ_p is the relaxation time for the pth normal mode, ζ the monomeric friction coefficient, and N the number of chain segments with bond length b. Since N is proportional to the molecular weight M_w, the Rouse theory predicts for the longest relaxation time

$$\tau_1 \propto M^{2.0} \qquad (6)$$

Numerical and analytical evaluation[18,19] of the discrete Rouse spectrum of a diblock A-B revealed strong dependence on composition and the friction coefficient ratio ζ_A/ζ_B. The boundary conditions[19] at the junction point for copolymers resemble those advanced in treating the normal-mode behavior of branched polymers. For a symmetric block copolymer, the longest relaxation time of one block approaches 4 times the corresponding relaxation time of the equivalent homopolymer. This corresponds to a tethered chain in a separated block copolymer. Analogous calculation of the normal-mode spectrum of A-B with thermodynamic interactions ($\chi N \neq 0$) is so far not known. In this context, the usual neglect of interchain correlations in eq 2 has to be questioned.

The spectrum of the segmental relaxation times for diblock copolymer melts[5,6] with $\chi N < (\chi N)_s$ was found to be significantly broader than that for the constituent bulk homopolymers due to the presence of adequate composition fluctuations within the cooperative volume V_g associated with the glass transition. For homopolymer blends the broadening of the distribution function has recently been discussed in terms of the coupling scheme of relaxation[20] and a concentration fluctuation approach.[21]

Table I
Molecular Characteristics of the PS-*b*-PI Samples[a]

sample	PI (wt %)	f_{PI}	M_n(PS)	M_n(total)	T_g (K)	χN at 25 °C
SI-4	27.9	0.37	2830	3930	308	5.5
SI-5	35.9	0.46	2830	4410	284	6.4
SI-6	50.4	0.61	2830	5700	255	8.9

[a] The interaction parameter χ is taken from ref 34.

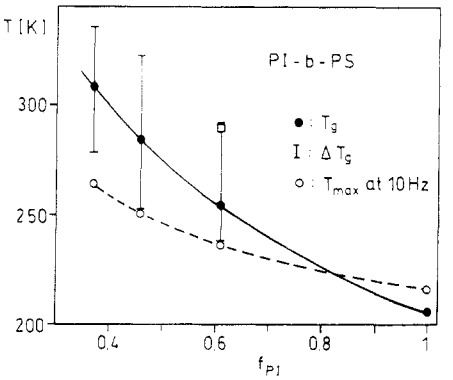

Figure 1. Variation of the glass transition temperature T_g and its breadth ΔT_g with the PI composition f_{PI} in the three block PI-*b*-PS copolymers. The open circles denote the temperature T_{max}, of maximum dielectric absorption ϵ'' at 10 Hz due to segmental relaxation in PI-rich regions. The square symbol (□) indicates the segmental relaxation in the PS-rich environment as measurement by DRS.[6]

III. Experimental Section

Samples. Three diblock copolymers poly(styrene-*b*-*cis*-1,4-isoprene) (PS-*b*-PI) were prepared by anionic polymerization.[22] The samples' characteristics are summarized in Table I. The glass transition T_g and its width (as determined calorimetrically at a heating rate of 20 K/min) depend strongly on the composition of the copolymer (Figure 1).

Dielectric Spectroscopy (DS). The dielectric measurements covered the frequency range from 10^{-2} to 10^6 Hz using a Solartron-Schlumberger frequency response analyzer FRA 1254. The sample was kept between two gold-plated stainless steel electrodes (diameter 20 mm), with a spacing of 50 ± 1 μm maintained by two fused silica fibers. By using a temperature-controlled nitrogen gas jet and a custom-made cryostat, temperature adjustment over a broad range was achieved. The accuracy in the determination of ϵ'' is ±5%; the resolution of the temperature measurement was ±0.01 K.[23]

For the quantitative analysis the generalized relaxation function according to Havriliak-Negami[24] is used:

$$\epsilon^*(\omega) = \epsilon_\infty + \frac{\epsilon_s - \epsilon_\infty}{(1 + (i\omega\tau)^\alpha)^\gamma} \qquad (7)$$

where α and γ are parameters ($0 \leq \alpha, \gamma \leq 1$) describing the

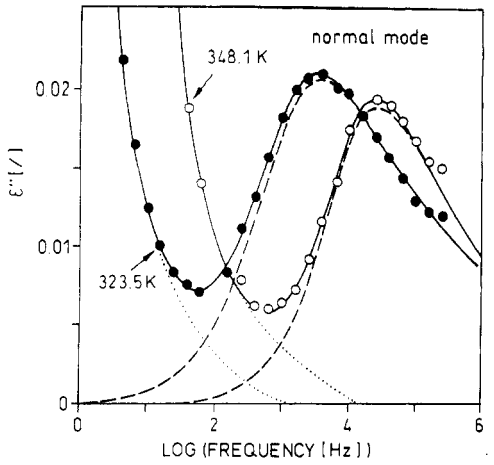

Figure 2. Dielectric absorption ϵ'' vs frequency for PI-*b*-PS with $f_{PI} = 0.61$ at two temperatures 348.1 and 323.5 K. The solid line is the superposition of the relaxation process (—) according to eq 7 and the conductivity contribution (· · ·) according to eq 8. The relaxation process (- - -) is assigned to the normal mode in PI.

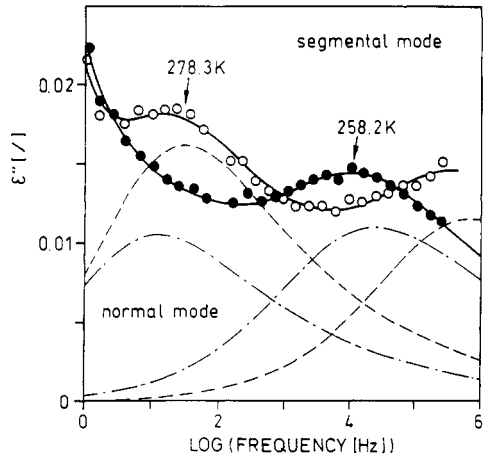

Figure 3. Dielectric absorption ϵ'' vs frequency for PI-*b*-PS with $f_{PI} = 0.61$ at two temperatures 278.3 and 258.2 K. The solid line indicates the superposition of two relaxation processes (278.3 K, ○; 258.2 K, ●), according to eq 7 and a conductivity contribution according to eq 8, which is not shown because of graphical reasons. The low-frequency process is assigned to the normal mode and the high-frequency process to the segmental mode (– · –, 258.2 K; - - -, 278.3 K).

symmetric and asymmetric broadening of the relaxation time distribution, τ is the relaxation time, and $\Delta\epsilon = \epsilon_s - \epsilon_\infty$ is the dielectric strength. On the low-frequency side, an additional conductivity contribution is superimposed, obeying a power law

$$\epsilon''(\omega) = \frac{\sigma_0}{\epsilon_0 \omega^{s-1}} \tag{8}$$

where σ_0 and s are fit parameters ($0 \le s \le 1$). ϵ_0 denotes the permittivity of free space. Using eqs 7 and 8 allows us to describe the data within experimental accuracy (Figure 2). In cases (Figure 3) where two relaxation processes overlap, two Havriliak–Negami functions have to be employed. The accuracy in the determination of the fit parameters α and γ is ±0.05 and in τ and $\Delta\epsilon$ ±10%. In most cases a fit for the segmental relaxation in the frequency domain was not possible without considerable ambiguity, especially when the segmental process had closely merged with the conductivity contribution and the normal mode. In these cases the temperature dependence of the relaxation time τ was determined from the temperature position of maximum loss at fixed frequency, assuming $\omega\tau = 1$. A determination of the distribution parameters α and γ was not possible under these conditions.

IV. Results and Discussion

The two dielectric absorption processes observed in the frequency domain (Figure 3) show up more clearly in their

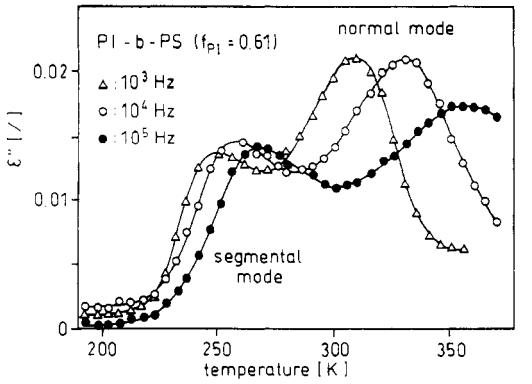

Figure 4. Dielectric absorption ϵ'' vs temperature at 10^4 Hz for three different compositions of PI-*b*-PS.

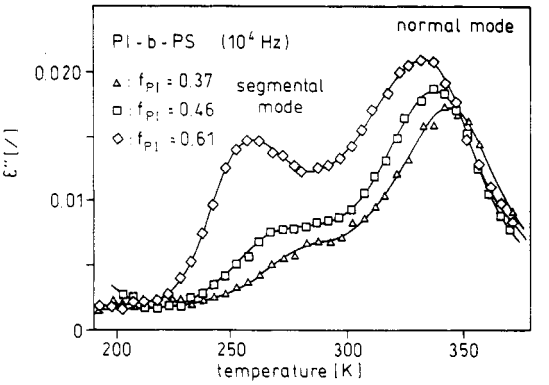

Figure 5. Dielectric absorption ϵ'' vs temperature at different frequencies for PI-*b*-PS with $f_{PI} = 0.61$.

temperature dependence (Figures 4 and 5). These processes are assigned to the segmental and normal modes which originate in the perpendicular and the parallel component of the net dipole moment of a monomer unit of PI. The segmental mode corresponds to a local relaxation process in which only a few monomer units are involved,[25] while the normal mode shows a pronounced molecular weight dependence. Both processes strongly depend on the composition of the diblock copolymer in their frequency response temperature position and in their width. The α-relaxation in PS is dielectrically active as well. Its dielectric strength is about 2 times smaller than that of the segmental or the normal mode of PI. This would lead to a factor of about 4 in ϵ''. Thus, if the PS and the PI relaxations would be superimposed in the temperature and frequency window where the molecular dynamics of the diblock copolymers has been analyzed, one would have to expect either a bimodal or at least a strongly broadened relaxation time distribution. Concerning the normal-mode relaxation, it cannot be ruled out that for the sample SI-6 at a temperature between 290 and 320 K two processes add up, but in the spectra no shoulder and no additional broadening was observed. Hence, it is concluded that the primary relaxation in PS and the PI relaxations are not superimposed in the dielectric spectra.

Segmental-Mode Relaxation. The segmental-mode relaxation in the PI–PS block copolymers exhibits a temperature dependence similar to that in the bulk PI homopolymer (Figure 6). It is located closer to the relaxation time of the PI homopolymer than expected from the PI content in the block copolymer. This indicates that this local relaxation process occurs within the PI-rich region. Its microscopic friction coefficient should be determined by the composition of these regions in the block copolymer. For the quantitative analysis the Vogel–Fulcher–Tamann–Hesse (VFTH) equation is used to describe the temper-

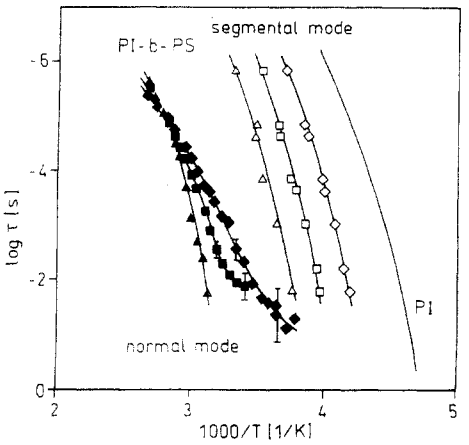

Figure 6. Arrhenius plot of the relaxation times τ_n and τ_s respectively for the normal-mode and segmental-mode processes in the three PI-*b*-PS copolymers with $f_{PI} = 0.37$ (△), 0.46 (□), and 0.61 (◇). The solid line denotes the τ_s for the bulk PI homopolymer having a molecular weight of $M_w = 5100$.[12]

Table II
VFTH Parameters As Determined from Equation 9 for the Normal and Segmental Modes

sample	$-\log [\tau_0$ (s)]	B (K)	T_∞ (K)
	Normal Mode		
SI-4	10.4	537	258
SI-5	9.5	556	234
SI-6	8.9	610	200
PI	5.9	536	166
	Segmental Mode		
SI-4	12.5	634	208
SI-5	12.8	638	194
SI-6	12.6	583	185
PI	12.3	456	170

ature dependence of τ_s:

$$\tau_s = \tau_0 \exp[B/(T - T_\infty)] \quad (9)$$

where τ_0 is the relaxation time at infinitely high temperature, B an activation parameter, and T_∞ the ideal glass temperature (Table II).

To analyze the composition dependence of the segmental relaxation times τ_s (Figure 6), we calculated the WLF coefficient C_2, which should be constant if T_∞ scales with T_g of the copolymer. From the parameters $T_\infty = T_g - C_2$ (Table II) and T_g (Table I), the WLF coefficient C_2 is calculated to vary systematically from 70 to 100 K for PI-*b*-PI with $f_{PI} = 0.61$ and 0.37, respectively; for bulk PI, $C_2 = 40$ K. This variation of C_2 with f_{PI} is due to the stronger composition dependence of the DSC-determined T_g compared to T_∞. The situation is also illustrated in a plot where T_{max} (at which $\epsilon''(\omega,T)$ due to the segmental mode in PI-*b*-PI exhibits a maximum at 10 Hz) is compared to T_g (Figure 1). In spite of the fact that the determination of T_g from the broad DSC curves of the copolymer is subject to a rather large error, T_{max} and the calculated $T_g^*(f_{PI}) = T_\infty(f_{PI}) + C_2(PI)$ for the PI-rich environment exhibit a weaker composition dependence than the T_g in the bulk copolymer. Moreover, the values of T_{max} and T_g^* lie near the lowest edge of the breadth ΔT_g.

Further evidence for the influence of slow composition fluctuations on the segmental dynamics arises from DRS measurements[6] on the block copolymer SI-6. While the dielectric measurements are probing segmental motion in the PI-rich region, DRS measures the segmental relaxation in the PS-rich environment. For the sample SI-6 the two segmental relaxations are (at 10 Hz) 54 K apart. It is noteworthy that the segmental relaxation of the PS-rich region is located at the upper limit of the glass transition region (square symbol in Figure 1). The observation of two distinct primary relaxation processes for the homogeneous PI-*b*-PS samples supports the fluctuation picture[3] of block copolymers for temperatures above MST. Since the composition correlation length ξ, which is at least on the order of the size (~20 Å) of the copolymer chain, usually exceeds the cooperative length $\sim V_g^{1/3}$ associated with the glass transition,[26,27] the splitting into two distinct segmental processes can be rationalized.

Table III
Havriliak-Negami (Equation 7) Fit Parameters for the Normal and Segmental Modes[a]

T (K)	$\Delta\epsilon_{HN}$	τ_{HN}	α	γ	β_{KWW}
		Normal Mode			
348	0.083	1.7×10^{-5}	0.86	0.33	0.37
338	0.092	3.7×10^{-5}	0.82	0.33	0.35
328	0.10	9.8×10^{-5}	0.80	0.31	0.32
318	0.10	2.4×10^{-4}	0.70	0.37	0.31
308	0.11	7.0×10^{-4}	0.60	0.44	0.34
298	0.12	2.5×10^{-3}	0.56	0.44	0.32
		Segmental Mode			
263	0.10	2.3×10^{-5}	0.42	0.38	0.25
253	0.061	8.2×10^{-5}	0.57	0.38	0.29
243	0.081	3.6×10^{-3}	0.48	0.38	0.25

[a] Sample: SI-6. β_{KWW} is the "stretched" exponential according to Kohlrausch, Williams, and Watts.[16]

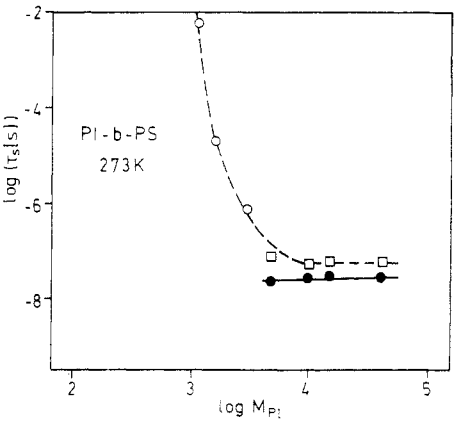

Figure 7. Segmental relaxation times for the PI block vs molecular weight M_{PI} of the PI sub(chain) in homogeneous (○) and heterogeneous (□)[13] PI-*b*-PS block copolymers. The filled symbols denote τ_s in bulk PI homopolymers.[13]

From the fits in the frequency domain the distribution parameters α and γ can be determined (Table III). The parameter α describing the symmetric broadening of the distribution of relaxation times is much smaller than in the case of the PI homopolymer; for a sample with $M_w = 17\,200$, $\alpha = 0.62$, $\gamma = 0.66$, and $\beta_{KWW} = 0.39$ at $T = 254$ K.[12] Hence, the distribution of relaxation times is strongly broadened in the block copolymers. In view of the composition fluctuations this result is not unexpected.[21]

Recently, segmental relaxation times of PI block in microphase-separated PI-*b*-PS block copolymers and the corresponding PI precursors were measured by DS.[13] Figure 7 depicts the variation of τ_s with the molecular weight M_{PI} of the PI block or homopolymer. For comparison the present τ_s values for the homogeneous PI-*b*-PS samples are also shown in Figure 7. As expected, the local relaxation times τ_s for the microphase-separated PI-*b*-PS samples are insensitive to M_{PI} variation, similar to that in PI homopolymers; in the segregated state the PI segments are assumed to behave in a manner similar to that of the homopolymer. In contrast, the present non-microphase-separated ($\chi N < (\chi N)_s$) copolymers display a different behavior; the increase in τ_s for M_{PI} below 4×10^3 indicates the crossover to the homogeneous regime. The slowing

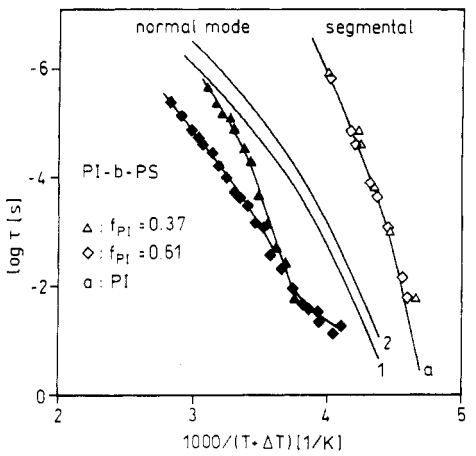

Figure 8. Reduced plot of the normal- and segmental-mode relaxation times in PI-*b*-PS block copolymer. The times for two copolymers were shifted on the T axis by ΔT = 52.4 and 21 K respectively for the sample with f_{PI} = 0.37 and 0.61. The solid curves 1 and 2 denote the relaxation time for the first normal mode of equivalent PI homopolymers[12] according to eq 5. Curve 1: N_{PI} = 69. Curve 2: N_{PI} = 43. (Because of graphical reasons, the data for f_{PI} = 0.46 are omitted.) The solid line marked by a is the segmental mode in the PI homopolymer (M_w = 5100).

down of τ_s with decreasing M_{PI} follows the increasing microscopic glass transition temperature T_g* of the PI-rich regions.

Normal-Mode Relaxation. In contrast to the segmental-mode relaxation, the normal-mode relaxation exhibits—compared to homopolymers—a completely different frequency and temperature dependence in block copolymers (Figure 6). In order to normalize the data with respect to the local friction coefficient as sensed by the segmental-mode relaxation, the data are shifted on the temperature axis: Shifts of 21, 35, and 52.4 K lead to a superposition of the segmental relaxation times of PI-*b*-PS respectively with f_{PI} = 0.61, 0.46, and 0.37 with τ_s of the bulk PI homopolymer (M_w = 5100 from Figure 4 of ref 12) as shown in Figure 8 for two of the samples. Again these temperature shifts are smaller than the corresponding differences in T_g of PI-*b*-PS and PI (49, 79, and 102 K). Whereas superposition is observed for τ_s in block copolymers and bulk PI, the temperature dependence of τ_n shows the following features: (i) In comparison to PI homopolymers (curves 1 and 2) of equivalent chain lengths, the relaxation times are strongly increased in the copolymers. (ii) The separation between τ_n and τ_s ("breadth" of the relaxation time spectrum) has a different temperature dependence compared to the PI homopolymer and depends on the PI block length. (iii) At low temperatures the temperature dependence of τ_n deviates from the VFTH behavior. (iv) The distribution of the relaxation function is much broader in the block copolymers (Table III) than in the homopolymer.

As stated in (i), the time scales characteristic for segmental motion of PI and normal-mode relaxations of copolymer chains are separated more than we would anticipate for a PI chain of the same length in the bulk state. For comparison we have computed the relaxation time τ_1 for the first normal mode of the PI blocks in the copolymer chain using the relaxation time of bulk PI (M_w = 5100, ref 12) assuming a N^2 dependence (eq 6). The curves 1 and 2 in Figure 8, for N_{PI} = 69 and N_{PI} = 43, respectively, refer to the local friction coefficient of the bulk PI (curve a). Therefore, the additional slowing down of the normal-mode relaxation times τ_n observed in the disordered phase of diblock copolymers can be due to the differences in the monomeric friction coefficient of foreign blocks.

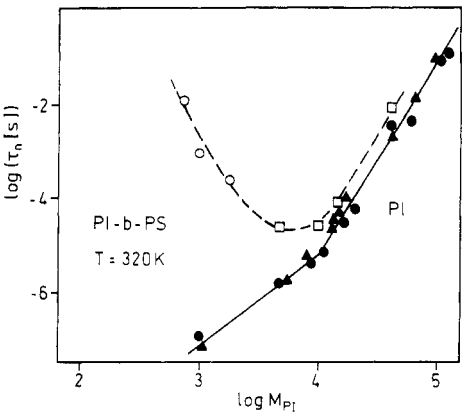

Figure 9. Normal-mode relaxation times vs molecular weight M_{PI} of the PI (sub)chain for homogeneous (○), heterogeneous (□), ref 13 and PI bulk homopolymers (solid symbols): ●, ref 11; ▲, ref 12. The broken line is a guide to the eye.

As predicted earlier,[18,19] the normal-mode spectrum of athermal homogeneous block copolymers (for free-draining conditions) depends sensitively on block composition and the friction coefficient ratio ζ_A/ζ_B, where B is the mobile component (here PI). For a block composition f_B = 0.5, a ratio of $\zeta_A/\zeta_B \sim 200$ can cause a similar slowing down of the normal-mode relaxation time as observed for sample SI-6. Though the former numerical result offers a quantitative account for the pertinent experimental finding, a qualitative description is precluded mainly because the value of ζ_A/ζ_B and chain dimensions to be assigned to the blocks are not known. Whereas the segmental relaxation times being a measure of a local friction coefficient referred to regions rich in one of the blocks, the end-to-end fluctuations of the PI-*b*-PS chain with comparable dynamics and lengths scales as the fluctuating composition pattern are dominated by a friction coefficient averaged over different regions.

The effective friction coefficient for the chain motions is expected to be between the friction coefficients of the PS- and PI-rich regions of the copolymer. To explain the different temperature dependence of τ_n for the different copolymer compositions, a temperature-dependent effective friction coefficient, which differs for the different compositions, has to be assumed. A possible reason for this finding might be the neglect of the thermodynamic interactions expressed by different χN in Table I. Furthermore, the χN values are temperature dependent, which leads to an increase of the composition fluctuations with decreasing temperatures. The slowing down of the reduced τ_n for SI-4 compared to SI-6 (Figure 8) indicates the different coupling between composition fluctuations and normal-mode dynamics for different thermodynamic interactions. A further indication for the coupling of normal-mode dynamics and composition fluctuation is the broadening of the normal-mode relaxation of the copolymers (Table III) compared to the homopolymers ($\beta_{KWW} \simeq 0.5$–0.7[12]).

The observed kink (iii) in the temperature dependence of τ_n for samples SI-5 and SI-6 at low temperatures may be attributed to a freezing-in of the PS segmental motions, whereas the segmental dynamics in PI-rich regions is unaffected. This is supported by a comparison of DR and DSR measurements[6] on sample SI-6, where it is shown that at low temperatures the segmental dynamics in the PS-rich region becomes slower than τ_n of the PI blocks. In this case we have to expect normal-mode dynamics of the flexible PI blocks in a structure of frozen-in PI blocks.

In Figure 9 our τ_n values are compared to those of microphase-separated copolymers[13] having higher molecular weights and to results for PI homopolymers.[11,12] The

τ_n from ref 13 were shifted by the factor a_T given in the same paper to reduce all data to 320 K. As discussed before, in the case of microphase separation ($\chi N > (\chi N)_t$), it is important to consider a tethered type A Gaussian chain and, similar to star-shaped polymers,[28-30] the longest relaxation time should be 4 times longer than that of a free Gaussian chain of the same length. The experimental finding that τ_n for the microphase-separated samples is about a factor 3–4 slower than those of their PI precursors seems to be in agreement with this prediction, although the broadening of the normal-mode distribution needs further explanation.[13] Below $M_{PI} \sim 10^4$ the normal-mode relaxation time deviates totally from the power law observed in the microphase-separated block copolymers and in the homopolymer (Figure 9). This reflects an observation similar to that in Figure 7 for the segmental-mode relaxation showing the crossover from the microphase-separated to the homogeneous regime with decreasing M_{PI}.

Chain Conformation. The fits according to eq 7 (see Table III) deliver besides the relaxation time τ and the shape parameters α and γ the dielectric strength for the segmental- and normal-mode relaxation in the PI blocks. The segmental relaxation in the diblock copolymers exhibits—normalized to the PI content—a dielectric strength similar to that of PI homopolymers (for M_w = 17 200; $\Delta\epsilon_s(PI) \simeq 0.091$ at 254 K[12]). This indicates that the microstructure in the diblock copolymers and in the PI homopolymers used in ref 12 was comparable. Within experimental accuracy, the segmental-mode dielectric strength scales with the PI content. In contrast, the normalized dielectric strength $\Delta\epsilon_n/f_{PI}$ for the normal mode in the block copolymers exceeds strongly the corresponding dielectric strength for the homopolymer ($\Delta\epsilon_n(PI) = 0.085$ at 324 K[12]), and it depends only weakly on the PI composition. (This can qualitatively be seen already in Figure 5.) The normal-mode relaxation strength $\Delta\epsilon_n$ can be expressed by the formula

$$\Delta\epsilon_n = \frac{N_A \tilde{\mu}^2 \langle r^2 \rangle f_{PI}}{3 k_B T M_{PI}} \tag{10}$$

where N_A is Avogadro's number, $\tilde{\mu}$ is the dipole moment per unit contour length, M_{PI} is the molecular weight of the PI block, and $\langle r^2 \rangle$ is the root-mean-square distance of the PI block in the copolymer. Hence, the comparison between $\Delta\epsilon_n$(PI-*b*-PS)/f_{PI} and $\Delta\epsilon_n$(PI) proves that the PI block in the copolymer is expanded in the disordered phase near MST. A similar deviation of the static structure factor of a PI-*b*-PS diblock copolymer from the Gaussian coil assumptions was found recently[32] for temperatures near the MST using SAXS and dynamic experiments. It was also suggested by recent Monte Carlo simulations.[33] Blocks with larger chains are necessary to prove this interesting effect in more detail.

V. Conclusions

By comparison of dielectric relaxation measurements on thermodynamically homogeneous isoprene–styrene block copolymers to recently published data for samples which are microphase separated, significant changes in the normal-mode (τ_n) as well as segmental-mode (τ_s) dynamics at the microphase-separation transition (MST) were found. The existence of two dielectric active relaxations allowed us to differentiate between two length and time scales in the so-called homogeneous phase of a block copolymer. From the different composition dependence of τ_n and τ_s it was possible to give further evidence for composition fluctuations in the disordered phase of block copolymers and to test the length and time scales of those fluctuations.

The slight composition dependence of the segmental relaxation τ_s compared to the T_g dependence indicates the existence of PI-rich regions in the homogeneous phase larger than the length scale of the rearrangements connected to the main transition. The lifetime of those regions must, therefore, also be longer than the relaxation time (τ_s). The normal modes are assumed to be influenced mainly by an effective friction coefficient, which reflects the properties of both components. On the other hand, there are several indications for interaction between normal modes and composition fluctuations. The length and time scales of both seem to be comparable. Therefore, we assume that the composition fluctuations are originated in (or coupled to) the subchain dynamics.

Acknowledgment. I.A. is grateful for the hospitality of the Max-Planck-Institut für Polymerforschung in Mainz and the support by the Max-Planck-Gesellschaft. G.F. thanks Dr. S. Anastasiadis for helpful discussions. Financial support by the German Science Foundation in the framework of the SFB 262 is highly acknowledged.

References and Notes

(1) Bates, F. S.; Fredrickson, G. H. *Annu. Rev. Phys. Chem.* **1990**, *41*, 525 and references therein.
(2) Leibler, L. *Macromolecules* **1980**, *13*, 1602.
(3) Fredrickson, G. H.; Helfand, E. J. *J. Chem. Phys.* **1987**, *87*, 697.
(4) Quan, X.; Johnson, G. E.; Anderson, E. W.; Bates, F. S. *Macromolecules* **1989**, *22*, 2456.
(5) Kanetakis, J.; Fytas, G.; Kremer, F.; Pakula, T. *Macromolecules* **1992**, *25*, 3484.
(6) Fytas, G.; Alig, I.; Rizos, A.; Kanetakis, J.; Kremer, F.; Roovers, J. *Polym. Prepr. (Am. Chem. Soc., Div. Polym. Chem.)* **1992**, *33*, 86.
(7) Bates, F. S.; Rosedale, J. H.; Fredrickson, G. H. *J. Chem. Phys.* **1990**, *92*, 6255.
(8) Akcasu, A. Z.; Benmouna, M.; Benoit, H. *Polymer* **1986**, *27*, 1935.
(9) Onuki, A. *J. Chem. Phys.* **1987**, *87*, 3692.
(10) Bauer, M. E.; Stockmayer, W. H. *J. Chem. Phys.* **1965**, *43*, 4319.
(11) Adachi, K.; Kotacha, T. *Macromolecules* **1985**, *18*, 466.
(12) Boese, D.; Kremer, F. *Macromolecules* **1990**, *23*, 829.
(13) Yao, M.-L.; Watanabe, H.; Adachi, K.; Kotaka, T. *Macromolecules* **1991**, *24*, 2955.
(14) Cole, R. H. *J. Chem. Phys.* **1965**, *42*, 637.
(15) Nee, T.-H.; Zwanzig, R. *J. Chem. Phys.* **1970**, *52*, 6353.
(16) Williams, G. *Chem. Soc. Rev.* **1977**, *7*, 89.
(17) Rouse, P. E. *J. Chem. Phys.* **1953**, *21*, 1272.
(18) Hansen, D. R.; Shen, M. *Macromolecules* **1975**, *8*, 343.
(19) Stockmayer, W. H.; Kennedy, J. W. *Macromolecules* **1975**, *8*, 351.
(20) Roland, C. M.; Ngai, K. L. *Macromolecules* **1991**, *24*, 4261.
(21) Fischer, E. W.; Zetsche, A. *Polym. Prepr. (Am. Chem. Soc., Div. Polym. Chem.)* **1992**, *33*, 78.
(22) Toporowski, P. M.; Roovers, J. I. L. *J. Polym. Sci., Polym. Chem. Ed.* **1976**, *14*, 2233.
(23) Kremer, F.; Boese, D.; Meier, G.; Fischer, E. W. *Prog. Colloid Polym. Sci.* **1989**, *80*, 129.
(24) Havriliak, S.; Negami, S. *Polymer* **1967**, *8*, 161.
(25) Bahar, I.; Erman, B.; Kremer, F.; Fischer, E. W. *Macromolecules* **1992**, *25*, 816.
(26) Schick, C.; Donth, E. *Phys. Scr.* **1991**, *43*, 423.
(27) Matsuoka, S.; Quan, X. *Macromolecules* **1991**, *24*, 2770.
(28) Yoshida, H.; Adachi, K.; Watanabe, H.; Kotaka, T. *Polym. J.* **1989**, *21*, 863.
(29) Boese, D.; Kremer, F.; Fetters, J. *Polymer* **1990**, *31*, 1831.
(30) Boese, D.; Kremer, F.; Fetters, J. *Macromolecules* **1990**, *23*, 1826.
(31) Stockmayer, W. H.; Baur, M. E. *J. Am. Chem. Soc.* **1964**, *86*, 3485.
(32) Hoffmann, A.; Koch, T.; Schuler, M.; Stickel, F.; Stühn, B., submitted to *Prog. Colloid Polym. Sci.*
(33) Fried, H.; Binder, K. *J. Chem. Phys.* **1991**, *94*, 8349.
(34) Mori, K.; Hasegawa, H.; Hashimoto, T. *Polym. J.* **1985**, *17*, 799.

Registry No. PS-*b*-PI, 105729-79-1.